H_2 Superexcited States: Experimental and Theoretical Characterization of their Competing Decay-Channel Fluorescence, Dissociation, and Ionization

M. Glass-Maujean
Laboratoire de Physique Moléculaire pour l'Atmosphère et l'Astrophysique, Université Pierre et Marie Curie, 4 place Jussieu, 75252 Paris Cedex 05, France

Ch. Jungen*
Laboratoire Aimé Cotton du CNRS, Bâtiment 505, Université de Paris-Sud, F-91405 Orsay, France

H. Schmoranzer
Fachbereich Physik, Technische Universität Kaiserslautern, D-67653 Kaiserslautern

A. Knie, I. Haar, R. Hentges, W. Kielich, K. Jänkälä, and A. Ehresmann
Institut für Physik, Universität Kassel, D-34132 Kassel, Germany
(Received 18 December 2009; published 6 May 2010)

The absolute cross sections for the competing decay channels fluorescence, dissociation, and ionization of photoexcited long-lived superexcited H_2 molecular levels have been measured from the ionization threshold of H_2 up to the $H(1s) + H(n = 3)$ dissociation limit. The total and partial natural widths of these levels have been determined. Good agreement is found with first principles calculations carried out by multichannel quantum defect theory. The calculations reproduce the balance between the competing decay processes as well as its substantial level-to-level evolution.

DOI: 10.1103/PhysRevLett.104.183002 PACS numbers: 33.20.Wr, 33.50.Dq, 33.80.Eh, 33.80.Gj

Diatomic hydrogen H_2 is the most abundant molecular species in the Universe and it is the only molecule that is known to fluoresce when excited above its ionization energy [1,2]. This decay by fluorescence competes with slow ionization and dissociation decays which take place on the nanosecond scale. In astrophysics this emission is important as it contributes significantly to the extreme ultraviolet emission spectra of H_2, observed for instance in outer planet atmospheres [3]. Quantitative data on cross sections for all decay channels are unfortunately still missing for these astrophysical applications [4]. Here we present the first joint complete quantitative experimental investigation and theoretical treatment of the fluorescence decay $H_2^{**} \rightarrow H_2 + h\nu$ of the superexcited states and the competitively occurring dissociation and ionization decays, $H_2^{**} \rightarrow H(1s) + H(n = 2)$ and $H_2^{**} \rightarrow H_2^+ + e^-$. We show that (i) all three processes have significant cross sections, (ii) their relative importance varies substantially depending on which quasibound level is excited, (iii) the radiationless processes have a common origin, namely, weak nonadiabatic coupling between the electron and nuclear motions, leading to vibrational autoionization and electronic predissociation.

Figure 1(a) presents the fluorescence excitation spectrum of H_2 for energies ranging from the ionization threshold up to the $H(1s) + H(n = 3)$ dissociation limit. The spectrum was recorded by irradiating an H_2 sample (at 20 m Torr pressure, room temperature) with vacuum ultraviolet photons provided by the undulator beam line U125/2-10m-NIM at BESSY II (Berlin). The exciting photons were dispersed by a 10 m-normal-incidence monochromator equipped by a 1200 lines/mm grating [5,6] at a spectral resolution of 0.0012 nm (2 cm^{-1}). The fluorescence radiation was recorded using a visible sensitive detector. Figure 1(b) is a spectrum calculated from first principles by quantum defect theory (see below). The wavelengths of the experimental and theoretical spectra are seen to be in good agreement [7] [cf. inset of Fig. 1(a)]: with few

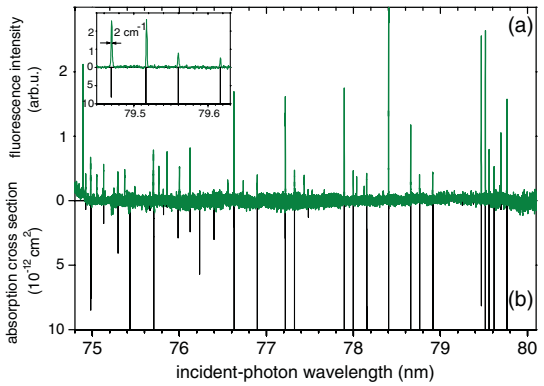

FIG. 1 (color). (a) Observed fluorescence excitation spectrum of superexcited levels of H_2 from threshold (ionization limit, 80.45 nm) to the $H(1s) + H(n = 3)$ dissociation threshold (74.84 nm). (b) Photoabsorption profile calculated from first principles by multichannel quantum defect theory. Inset: enlarged section.

exceptions there is a one-to-one correspondence between observed and calculated spectral lines, indicating that the calculated spectrum permits correct identification of the emitting superexcited molecular levels. The theoretical spectrum of Fig. 1 represents the *unconvolved* continuum absorption profile (no convolution with the experimental resolution width is made). The resonances that stand out in the calculation therefore are those which have the smallest calculated widths ($\Gamma/hc < 0.001$ cm^{-1}), and therefore the largest peak heights regardless of their *integrated* line intensity. The far more numerous broader resonances ($\Gamma/hc \approx 0.1$–10 cm^{-1}) are buried in the background. The calculations reveal that (with two exceptions not discussed here) all of the narrow resonances belong to a particular subset of molecular states, those having total parity $-(-1)^N$ where N is the total angular momentum of the molecule exclusive of spins. These levels are known to have $^1\Pi_u^-$ electronic symmetry, corresponding to a $p\pi$ Rydberg orbital that lies perpendicular to the rotational plane.

Figure 2 shows how the yields for the three competing processes, autoionization, predissociation, and molecular fluorescence have been determined experimentally for every spectral line shown in Fig. 1. Spectrum (a) represents the absolute absorption cross section. Spectra (b) and (c) show the excitation spectra for H_2^+ ion production and for atomic H fragment Lyman-α emission recorded simultaneously [6]. They were calibrated with respect to absorption by using broad resonances which appear only in ionization or only in dissociation, i.e., for which the ionization or dissociation yield is 100% (cf. the solid and dashed arrows in Fig. 2). The difference $\sigma_{\rm abs} - \sigma_{\rm ion} - \sigma_{\rm diss}$, panel (d), must then represent the remaining channel, the fluorescence excitation cross section $\sigma_{\rm fluo}$. Panel (e) displays the molecular fluorescence excitation spectrum recorded directly. The good agreement between panels (d) and (e) proves that the data sets are internally consistent. We use them now to deduce the decay yields for the superexcited levels of H_2.

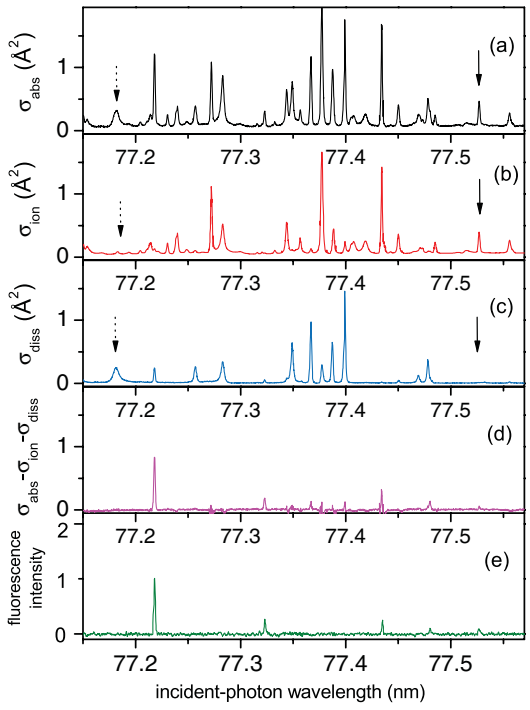

FIG. 2 (color). Excitation spectra of H_2 above the ionization threshold. The spectra (a)–(d) represent absolute cross section measurements. (a) photoabsorption, (b) photoionization, (c) photodissociation, (d) (a) − (b) − (c). (e) molecular fluorescence excitation spectrum recorded with a VIS sensitive detector.

By comparing the peak areas in spectra analogous to Fig. 2 for a number of peaks, we have determined the fluorescence, dissociation, and ionization yields of the $N = 1$ superexcited levels (+ parity) belonging to the $3p\pi D$, $4p\pi D'$, and $5p\pi D''$ Rydberg states of H_2 with vibrational quantum numbers ranging from 2 to 17. These results are displayed in Fig. 3. Fluorescence is seen to dominate for $n = 3$, whereas ionization takes over for higher electronic excitation, $n \geq 5$. $n = 4$ is a transition case. Dissociation is a minor component in all cases, but acquires a share of more than 10% for $n = 3$. A closer inspection of the data reveals that ionization takes over quite suddenly near $n = 4$, $v = 6$, and that the yields vary irregularly with v. The calculations indicate that this is due to nonadiabatic interactions affecting the $3p\pi$, $4p\pi$, and $5p\pi$ states. Indeed, the vibrational progressions of

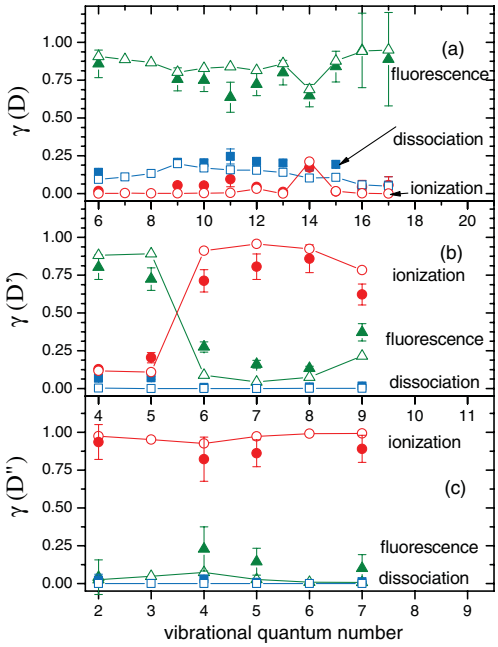

FIG. 3 (color). Fluorescence (triangles), dissociation (squares), and ionization yields (circles) for photoexcited superexcited levels of H_2 ($N = 1$, + total parity): (a) $3p\pi D$ state, (b) $4p\pi D'$ state, (c) $5p\pi D''$ state. Filled symbols: experiment; open symbols connected by lines: theory.

these electronic states are immersed in the $np\pi$, v Rydberg series with $n > 5$, which near the vibrational thresholds v^+ form dense Rydberg series causing perturbations. As Fig. 3 shows, theory accounts almost perfectly for the overall trends as well as for the detailed behavior. In the following we describe the theoretical approach.

The calculations were carried out using multichannel quantum defect theory MQDT [8], which is a generalized version of scattering theory, extended to include bound states (''closed'' channels) in addition to continua (''open'' channels). In the present problem two types of open channels arise, the nuclear dissociation continuum corresponding to relative motion of the dissociating H(1s) and H($n = 2$) atoms ($N = 1$ partial wave), and the electronic ionization continuum corresponding to the relative motion of the $p\pi$ photoelectron and the residual core H_2^+ $X\ ^2\Sigma_g^+(v^+, N^+ = 1)$ ($\ell = 1$ partial wave). The problem at hand therefore is equivalent to a reactive scattering situation, with a set of ionization continua corresponding to target vibrational states v^+, and a single vibrational continuum corresponding to the H_2 $2p\pi C$ state.

Standard frame-transformation MQDT accounts for nonadiabatic coupling within the Rydberg manifold of states through vibrational-electronic reaction matrix elements of the form [7,9,10]

$$K_{v^+v^{+\prime}} = \tan\left[\pi \int_0^{R_c} \chi_{v^+}(R)\mu(R)\chi_{v^{+\prime}}(R)dR\right], \quad (1)$$

where R is the internuclear distance, $\chi_{v^+}(R)$ and $\chi_{v^{+\prime}}(R)$ are ion vibrational wave functions coupled by vibronic interaction, and $\mu(R)$ is the R-dependent quantum defect characterizing the $p\pi$ Rydberg channel. For weak coupling (as here), the quantum defect may be evaluated from quantum-chemical clamped-nuclei potential energy curves by use of the Rydberg equation,

$$\mu(R) = n - (2^{-(1/2)})[U^+(R) - U_n(R)]^{-(1/2)}. \quad (2)$$

$U_n(R)$ is the potential energy curve (in a.u.) of the $np\pi$ Rydberg state, and $U^+(R)$ is the curve of the ion ground state. We used the *ab initio* curves $U_n(R)$ for $n = 2$–4 [11], permitting also inclusion of a slight energy dependence of $\mu(R)$ [7]. The vibrational wave functions and the integrals in Eq. (1) are evaluated in a *finite* range $0 \le R \le R_c$, thus defining a so-called ''R matrix'' at $R = R_c$. R_c is chosen ($\approx$8 bohr) such that the potential well $H_2^+X^2\ \Sigma_g^+$ is contained inside the boundary, and all bound H_2^+ vibrational levels E_{v^+} and associated wave functions up to $v^+_{\text{last bound}}$, the last bound level supported by the potential, are unaffected by this restriction.

MQDT procedures match the short-range wave functions implied by the reaction matrix $\mathbf{K}$ of Eq. (1) for a given total energy E, to asymptotically correctly behaving electron Coulomb wave functions by requiring [8]

$$\det|\mathbf{K} + \tan\boldsymbol{\beta}(E)| = 0. \quad (3)$$

$\boldsymbol{\beta}(E)$ is an asymptotic phase vector whose components $\beta_{v^+}(E)$ take different values depending on whether a Rydberg channel is closed ($E < E_{v^+}$) or open ($E > E_{v^+}$). For closed channels $\beta_{v^+}(E) = \pi\nu_{v^+}$ with $\nu_{v^+} = (2^{-(1/2)})[E_{v^+} - E)]^{-(1/2)}$ the effective principal quantum number corresponding to that channel. For open channels $\beta_{v^+}(E) = \pi\tau_\rho$, where $\pi\tau_\rho$ denotes the set of open-channel asymptotic eigenphases to be determined by solving Eq. (3) [8]. There are as many $\pi\tau_\rho$'s as there are ionization continua, i.e., thresholds E_{v^+} lower than E.

We proceed by solving Eq. (3) using three different types of vibrational basis: (i) Restriction of the basis v^+ to closed Rydberg channels which are vibrationally bound, $v^+_{\text{first closed}} \le v^+ \le v^+_{\text{last bound}}$ (with $v^+_{\text{first closed}}$ the electronically closed channel with lowest v^+), yields the discrete set of energies of the superexcited vibronically mixed Rydberg levels. It has been shown previously [7] that the line positions and absolute absorption intensities evaluated in this way from first principles are in good agreement with experiment. (ii) Inclusion of *all* vibrationally bound channels, $0 \le v^+ \le v^+_{\text{last bound}}$, thus including also the ionizing open Rydberg channels, yields absorption profile (Fig. 1) and the energy-dependent eigenphases from which the vibrational autoionization widths Γ_{ion} are extracted. (iii) Our treatment of dissociation [12] is based on the realization that the dissociating state $2p\pi C$ is simultaneously also the lowest member of the $p\pi$ ionization channel and as such plays a double role. This implies that the nonadiabatic coupling leading to vibrational autoionization of the $np\pi$ manifold above threshold is the same as that causing predissociation by the $2p\pi C$ state. Therefore the $K_{v^+v^{+\prime}}$ matrix elements of Eq. (1) contain *all* the information required to evaluate the predissociation widths in addition to the autoionization widths. We exploit this circumstance as follows: The vibrational wave functions χ_{v^+} and energies E_{v^+} are evaluated by using a ''large'' basis including only electronically bound Rydberg channels, $v^+_{\text{first closed}} \le v^+ \le v^+_{\text{large}}$, where $v^+_{\text{large}} \approx 3v^+_{\text{last bound}}$. The vibrational wave functions with $v^+ > v^+_{\text{last bound}}$ reach out to $R = R_c$. A common boundary condition $b = -\chi'/\chi$ is imposed on all $\chi_{v^+}(R)$ at $R = R_c$. With a ''large'' basis, the bound ion target levels remain at their correct energies, but the level spectrum E_{v^+} now extends beyond the bound range into the H_2^+ vibrational continuum where the energies depend on the particular boundary condition b used. Similarly, solution of Eq. (3) yields the Rydberg levels near their correct energies, but in addition a set of fictitious Rydberg levels with $n = 2$, $v^+ > v^+_{\text{last bound}}$ is obtained which represents the discretized $2p\pi C$ state vibrational continuum.

When the boundary condition b is varied, these levels may be tuned through the position of a bound Rydberg level with $n \ge 3$, $v^+ < v^+_{\text{last bound}}$. Vibronic interaction

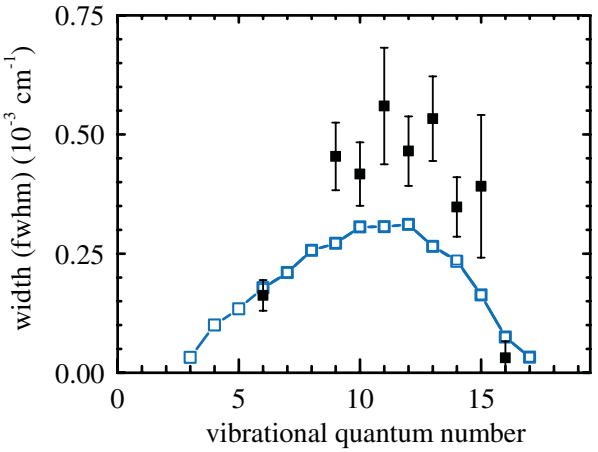

FIG. 4 (color). Dissociation widths $\Gamma_{\rm diss}/hc$ of $3p\pi\ D\,^1\Pi_u^-$ levels in H_2 ($N = 1$). Filled squares: experiment. Open squares connected by lines: first principles theory.

leads to an avoided crossing characterized by a closest approach $2V$. From this the predissociation width $\Gamma_{\rm diss}$ may be extracted using Fermi's golden rule $\Gamma_{\rm diss} = 2\pi V^2/\Delta E$, where ΔE^{-1} is the density of levels with $n = 2$, $v^+ > v^+_{\rm last\ bound}$. A variational formulation of this approach may be found in Ref. [13].

Finally, the natural widths corresponding to fluorescence, $\Gamma_{\rm fluo}$, are evaluated from the absorption cross sections calculated in [7], essentially by dividing the previously determined line strengths by the Franck-Condon factor. More precisely, the energy and R dependences of the dipole transition moments as well as the frequency factor for fluorescence must also be accounted for. Once the partial widths $\Gamma_{\rm ion}$, $\Gamma_{\rm diss}$, and $\Gamma_{\rm fluo}$ are evaluated for every superexcited level considered, the yields are obtained as, e.g., $\gamma_{\rm ion} = \Gamma_{\rm ion}/(\Gamma_{\rm ion} + \Gamma_{\rm diss} + \Gamma_{\rm fluo})$.

Since the absorption cross section is measured here on an absolute scale, the present data permit also the determination of the partial widths $\Gamma_{\rm ion}$, $\Gamma_{\rm diss}$, and $\Gamma_{\rm fluo}$ themselves, despite the fact that they are far smaller than the experimental resolution. This is again achieved, as above, in essence by dividing the previously determined [6] line strengths by the Franck-Condon factor. Figure 4 displays the vibronic predissociation widths thus obtained for the vibrational levels of the $3p\pi\ D\,^1\Pi_u^-$ state. The comparison with theory is satisfactory; note that these widths correspond to lifetimes on the scale of $>0.01\ \mu$s.

As far as we are aware, the present study is the very first where the three decay channels open to an isolated molecule have been studied by experiment and theory in a complete and unified manner and their competition characterized for numerous quantum levels. These processes are slow here, as they take place on the scale of a ns or longer. Despite its resolution, the experimental method is far from permitting direct access to the natural widths of the spectral lines. It is the measurement of absolute intensities which enables us to extract the molecular dynamics from the data. The theoretical method used here, multichannel quantum defect theory, is not widely used in the chemical physics community. We demonstrate that MQDT combined with accurate *ab initio* structure calculations [11], without any further adjustments, is capable of describing the nonadiabatic molecular dynamics in astonishing detail. We think, in conclusion, that the superfluorescing levels of molecular hydrogen and the radiative and nonradiative processes affecting them, are not only of importance for astrophysics, but also represent a textbook example of intramolecular dynamics in general.

M. G.-M. acknowledges help from the BESSY staff, especially G. Reichardt and A. Balzer, and EU support (Grant No. ELISA 226716). C. J. was supported in part by the ANR (France) under Contract No. 09-BLAN-020901. A. K. acknowledges support by the Otto-Braun Fonds (Germany). W. K., I. H., R. H., and A. E. acknowledge support by the DFG and BMBF (Germany, Contract No. 05KS7RK1). K. J. was partially supported by the Finnish Academy of Sciences.

*Also at Department of Physics and Astronomy, University College London, London WC1E 6BT, U.K.

[1] W. Sroka, Phys. Lett. A **28**, 784 (1969).
[2] J. Breton, P. M. Guyon, and M. Glass-Maujean, Phys. Rev. A **21**, 1909 (1980).
[3] M. Glass-Maujean *et al.*, Astrophys. J. Suppl. Ser. **180**, 38 (2009).
[4] W. Liu and A. Dalgarno, Astrophys. J. **462**, 502 (1996).
[5] G. Reichardt *et al.*, Nucl. Instrum. Methods Phys. Res., Sect. A, **467–468**, 462 (2001).
[6] M. Glass-Maujean *et al.*, J. Chem. Phys. **126**, 144303 (2007); Mol. Phys. **105**, 1535 (2007).
[7] M. Glass-Maujean and C. Jungen, J. Phys. Chem. A **113**, 13124 (2009).
[8] *Molecular Applications of Quantum Defect Theory* edited by C. Jungen (The Institute of Physics, Bristol and Philadelphia, 1996).
[9] U. Fano, Phys. Rev. A **2**, 353 (1970).
[10] C. Jungen and O. Atabek, J. Chem. Phys. **66**, 5584 (1977).
[11] L. Wolniewicz and G. Staszewska, J. Mol. Spectrosc. **220**, 45 (2003).
[12] C. Jungen and S. Ross, Phys. Rev. A **55**, R2503 (1997).
[13] A. Matzkin, C. Jungen, and S. C. Ross, Phys. Rev. A **62**, 062511 (2000).